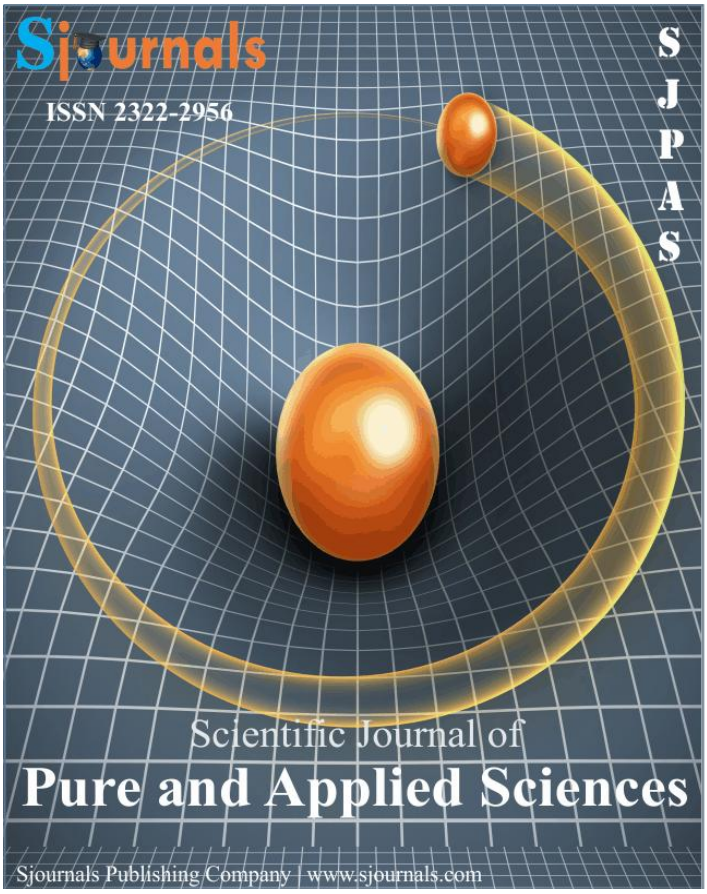

Scientific Journal of Pure and Applied Sciences (2016) 5(8) 476-482
ISSN 2322-2956
doi: 10.14196/sjpas.v5i8.2255

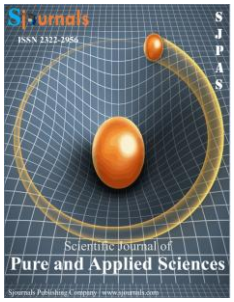

Contents lists available at Sjournals
Scientific Journal of **Pure and Appiled Sciences**
Journal homepage: www.Sjournals.com

Original article

Pyroelectric study of Mongolian tourmaline in electric power saving system by infrared spectroscopy

Ki-Seog Chang*
Biological and Chemical Engineering, Hongik University, 339-701, Korea.

*Corresponding author; Biological and Chemical Engineering, Hongik University, 339-701, Korea.

ARTICLE INFO

Article history,
Received 12 July 2016
Accepted 11 August 2016
Available online 18 August 2016
iThenticate screening 15 July 2016
English editing 09 August 2016
Quality control 15 August 2016

Keywords,
Tourmaline
X-ray diffraction
Pyroelectric
Infrared
Scanning electron microscopy

ABSTRACT

This Fourier Transformation Infrared (FTIR) experiment investigates the relevance of H_2O and other components' structural environments. The electronic power saving system in this study was compromised by four element materials: tourmaline, ferrite, NaCl, and H_2O. FTIR spectroscopy in the range of 3,000 to 4,000 cm^{-1} was then used to examine the hydroxyl ions of H_2O and tourmaline. The tourmaline crystal was found to be polar and therefore pyroelectric, electrical charges developing at the ends of the polar axis and the temperature changing from the IR activation with H_2O in the system. As a result, the tourmaline was shown to be related to the activation of H_2O as a pyroelectric substance.

1. Introduction

While lifestyles change quickly in the modern world, one constant is the increasing importance of energy. Providing energy in the face of fossil fuel shortages may heavily burden a nation's economy. The alternative of electric energy becomes popular, even necessary in certain industries. But electric energy comes with its own challenges: In order to provide reliable and economical electric energy, a highly efficient energy system is key (Halmlin, 2011). We study such a system here. The system in our research was comprised of four important materials: tourmaline, ferrite, salt (NaCl), and water (H_2O). The tourmaline serves as a basic material. The tourmaline radiates in the far infrared region as well as provides excellent thermoelectricity and piezoelectricity

(Dietrich, 1985; Castaneda et al., 2006). In the infrared experiment, the absorption peaks between 3000 cm^{-1} and 3600 cm^{-1} were attributable to the O-H band stretching the vibration of the structure and absorption of tourmaline and water for the pyroelectricity of tourmaline (Bour, 2002). Generally, the "free" O-H stretch showed a sharp peak appearing at 3600 to 3650 cm^{-1}, if no hydrogen bonding takes place. This stretch was observed only in dilute solutions. The hydrogen bonded O-H stretch was a broad peak that occurred more to the right at 3200 to 3500cm^{-1} (Pavia et al., 1979; Zhu et al., 2008; Krambrock et al., 2004).

In Fig. 1, we find that the peak appearing at 3559 cm^{-1} originated from the comparatively dilute, no hydrogen bonded hydroxyl-group (-O-H) of tourmaline (Pavia et al., 1979; Zhu et al., 2008; Krambrock et al., 2004). The other peaks, 3410 cm^{-1} and 3222 cm^{-1}, were the two broad peaks that occurred more to the right at 3200 to 3500 cm^{-1} with the hydrogen bonded O-H stretches. The 3222 cm^{-1} peak showed a more cooperative interaction in hydrogen bonding in comparison to the 3410 cm^{-1} peak. Thus, we found that the hydroxyl group ($H_3O_2^-$ ion) was determined at about 3222 cm^{-1} peak as a very broad O-H stretch vibration. The tourmaline powders were prepared by mixing ferrite materials with water as infrared materials (3000 cm^{-1} ~ 4000 cm^{-1}). The infrared emissivity of the morganite including tourmaline minerals ($(Na^+, Ca^{2+}, K^+)(Ti^{4+}, Fe^{3+}, Fe^{2+})(Al^{3+}, Mg^{2+})_6(SiO_3)_6(BO_3)_3(OH^-, F^-)_4$) in the power saving system depended upon the composition of the mixture and the structure of the materials. The mixing ratio and the infrared emission property of tourmaline and water (H_2O) were also examined in detail.

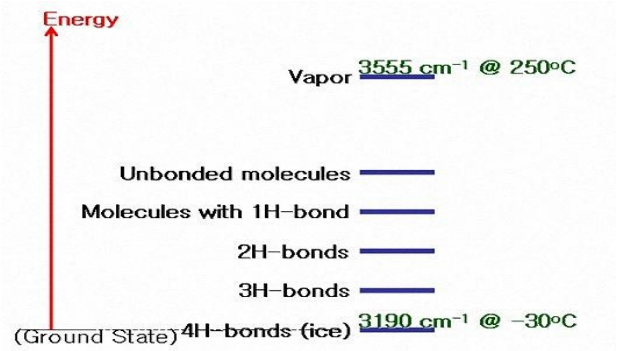

Fig. 1. Schematic representation of energy levels for H2O molecules in liquid water.

2. Experiment details

2.1. Characterization methods

2.1.1. XRD

The X-ray powder diffraction (XRD) analysis was performed on a Bruker AXS diffractometer that used CuKα monochromatic radiation (λ = 0.154056 nm) as its X-ray source. The patterns were scanned over the 2θ angular range of 10 to 60°, and matched with a graph generated by the computer program LAZY-PULVERIX (Yvon et al., 1997). The X-ray powder diffraction pattern indicated that the composition of the mixture was right for tourmaline in a power saving system.

2.1.2. SEM

The morphologies and elemental compositions of the structures were investigated using a Phillips 505 field emission scanning electron microscope (SEM), coupled with energy dispersive X-ray spectroscopy (EDX) analysis from Kevex Super 8000 Microanalyzer. All tourmaline powders were examined without Au coating. Micrographs of the powders were obtained by spreading the samples directly onto carbon tape.

2.1.3. FTIR

The infrared radiation spectra of the samples were tested using a Fourier transform infrared (FTIR), Bruker Optik GMBH with a blackbody furnace. Emissivity is the ratio of radiant emittance of an object to that of a blackbody. Here, we use the integral value ratio of the radiation spectra between 400 and 4,000 wave number (cm^{-1}) as a far infrared emissivity. The state of bonding of each element was characterized by FTIR spectra.

3. Results and discussion

3.1. Structures

The structure of tourmaline was first proposed by Donny and Buer in 1950 (Donny and Buerger, 1950; Choo, 2003). Since, the tourmaline mineral group has been considered one of the most chemically complicated groups of silicate minerals. The unit cell of tourmaline, (Na, Ca) (Li, Mg, Al)$_3$(Al, Fe, Mn)$_6$(BO_3)$_3$$Si_6O_{27}(OH, F)_4$, belongs to the rhombohedral crystal system and the space group R_{3m}. In this research, the local structure of the tourmaline, such as molecular vibration and rotation with a changing dipolar moment in the infrared region (400 ~ 4000 cm^{-1}; 2.5 ~ 25 μm), was ultimately more important than the global structure because of the focus on pyro-electricity. The structure contains the ring-shaped layers of Si_6O_{18} on the 3-fold axis and three planar groups of trigonal BO_3 in the sequence ABAB. The Li, Mg, and Al atoms are coordinated with four O atoms and two F atoms or OH groups on the center of an octahedron, respectively. The Al, Fe, and Mn elements are coordinated with five O atoms and one F atom or OH group on the center of an octahedron, respectively. The six coordinated bonds of these two types can be described as a link of ring shaped column of Si_6O_{18} group and trigonal BO_3, and Na and Ca atoms in a space between 3-fold axises.

We identified that the main structure of the mixtures was consistent with X-ray diffraction patterns of tourmaline (mindat.org). The results of XRD (X-ray diffraction) patterns, SEM (Scanning electron microscopy) images, and EDX (Energy dispersive X-ray spectroscopic analyses) spectrum are shown in Fig. 2. Furthermore, the structure of ferrite in the electric power saving system was a hexagonal-dihexagonal dipyramidal gray mineral containing strontinum and barium as a magneto-plumbite. The general formula can be written $M^{2+}O{\cdot}6Fe_2O_3$ in which M^{2+} equals Ba^{2+} and Sr^{2+} and the ratio of Ba^{2+}/Sr^{2+} is about 6/49. The structure of tourmaline is characterized as a point group of "3m". The point group induced a spontaneous polarization, which is temperature-dependent. A good perturbation probe changes in temperature that will induce a flow of charge to and from the surface. This is the pyroelectric effect. All polar crystals are pyroelectric, so the 10 polar crystal classes are sometimes referred to as the pyroelectric classes as shown systematically in Fig. 3.

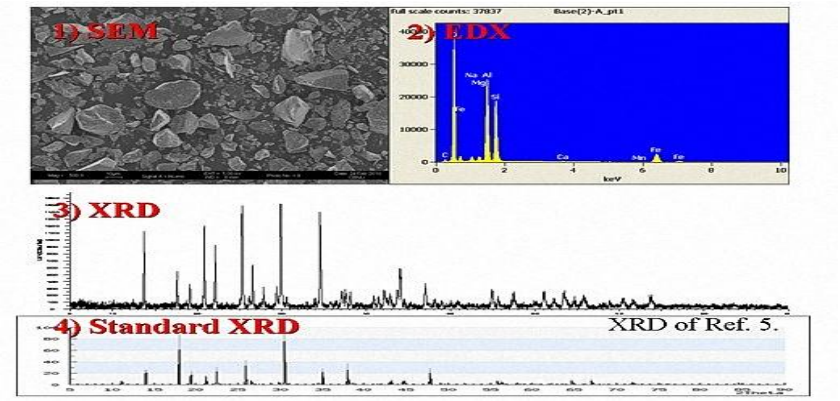

Fig. 2. 1) SEM, 2) EDX, 3) XRD, and 4) standard XRD9 of tourmaline, respectively.

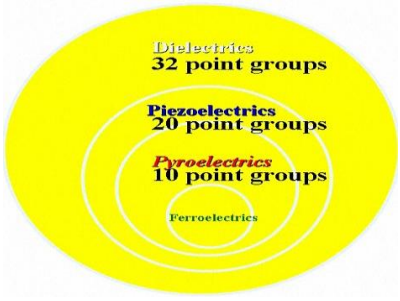

Fig. 3. Systematic diagram of the pyroelectric crystal classes.

3.2. Pyroelectrics

Based on the structural analyses with EDX and XRD data shown in Fig. 4, we analyzed the infrared spectra of Fig. 5, 6, 7, and 8. The absorption peaks between 900 and 1,200 cm^{-1} are attributed to the O-Si-O asymmetric stretching vibration in the ($[SiO_4]^{4-}$) group. The absorption peaks between 400 and 800 cm^{-1} are ascribed to Fe-O bond stretching vibration of the ($[Fe_2O_4]^{2-}$) group and the Si-O bond bending vibration and the Si-O-Si bonds symmetric stretching vibration of the ($[SiO_4]^{4-}$) group. Finally, the absorption peaks between 1,200 and 1,450 cm^{-1} are ascribed to the B-O bond asymmetric stretching vibration of the ($[BO_3]^{3-}$) group, and the relatively small peaks between 3,000 and 3,600 cm^{-1} are attributed to the O-H bond stretching vibration of the ($[OH]^{-}$) group in the structure and absorption of water. The absorption peak around 1840 cm^{-1} can be attributed to the O-H bond bending vibration. The FT-IR spectra are entirely derived from the structures of the tourmaline such as the global structure of trigonal (3m) crystal system and the local molecular structure.

IR spectra of tourmaline with and without water (H_2O) are shown in Fig. 4 and Fig. 5. Tourmaline, as shown in Fig. 3 and Fig. 4, display both piezoelectricity and pyroelectricity; tourmaline particles themselves have permanent polarity, which can be seen as an electric dipole. Because of the high electric fields from tourmaline nanoparticles, the hydrogen bonds of water were broken and rearranged continually and thus the water clusters became smaller (Sun et al., 2010). We experimented on four conditions: Tourmaline; Tourmaline and water; Tourmaline, water, and Ferrite; and Tourmaline, water, Ferrite, and NaCl. There were three important peaks, around 3559 cm^{-1} peak originated from Tourmaline, and around 3410 cm^{-1} and 3222 cm^{-1} peaks from water. We found that the water was activated by the mixtures of tourmaline, ferrite, and NaCl powders. The activation of water usually depended on the tourmaline.

As shown in Fig. 6, these findings were consistent with those of Fig. 4 and Fig. 5. The three peaks were separated using the Origin 8.0 program, which is a software application with data analysis and publication-quality graphing tools, including peak analysis, curve fitting, statistics, and signal processing (ORIGIN LAB. Origin 8.0 pro.). We found that the peak appearing at 3559 cm^{-1} originated from the comparatively dilute and no hydrogen bonded hydroxyl-group (-O-H) of tourmaline (Pavia et al., 1979; Zhu et al., 2008, Krambrock et al., 2004). As shown in the Fig. 8 summary, the delocalized electrons reallocated between the surface and increasing amount of water at 0g, 0.5g, 1g, 2g, and 8g H_2O with 5g-Tourmaline, or at 3g, 6g, and 8g-Tourmaline with 0.5g H_2O. The blue shift may be attributable to the stoichiometric effect, and not the generally thought surface or quantum effect.

In Table 2, the surface of the water that had been in contact with the tourmaline powder crystals changed in pH values (Sun et al., 2010), becoming approximately 9.9 as shown by pH experiments of 40ml H_2O and 5g tourmaline at 19.8^{o}C using a magnetic stirrer. These changes may also be explained by the occurrence of the electric field mentioned above in the IR experiments (Nishi et al., 1996; Nemethy and Scheraga, 1962; Bour, 2002).

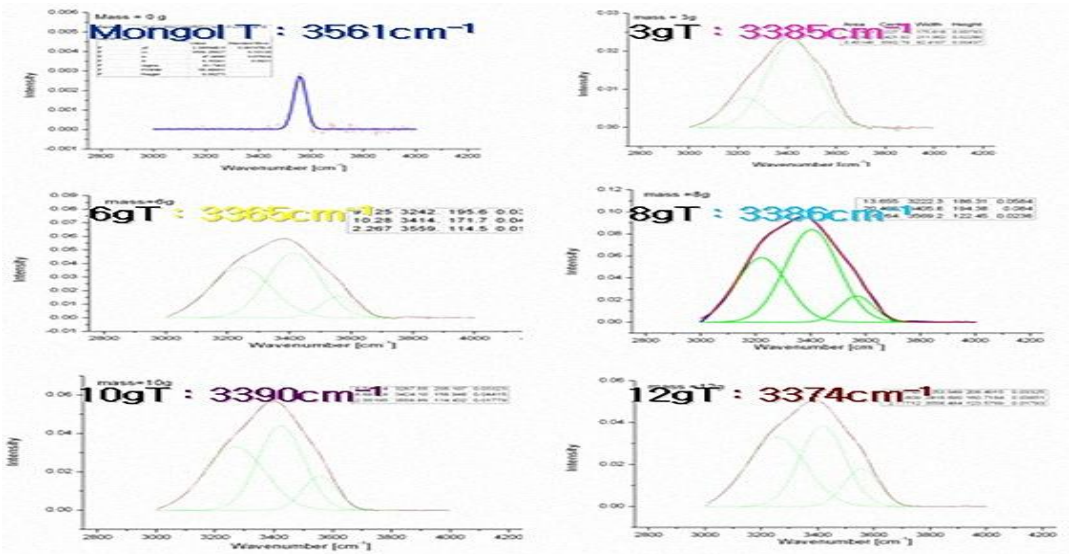

Fig. 4. Infrared Spectrum Absorbance (%) for increasing amounts of Tourmaline (0g; 3g; 6g; 8g; 10g; 12g) with 0.5g H2O.

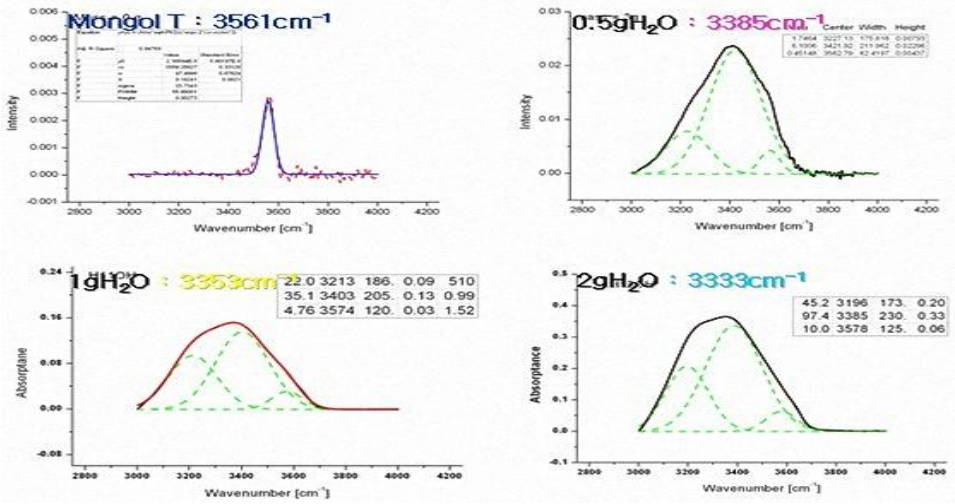

Fig. 5. Infrared Spectrum Absorbance (%) for increasing amounts of water(H2O) (0g; 0.5g; 1g; 2g) with 5g Tourmaline.

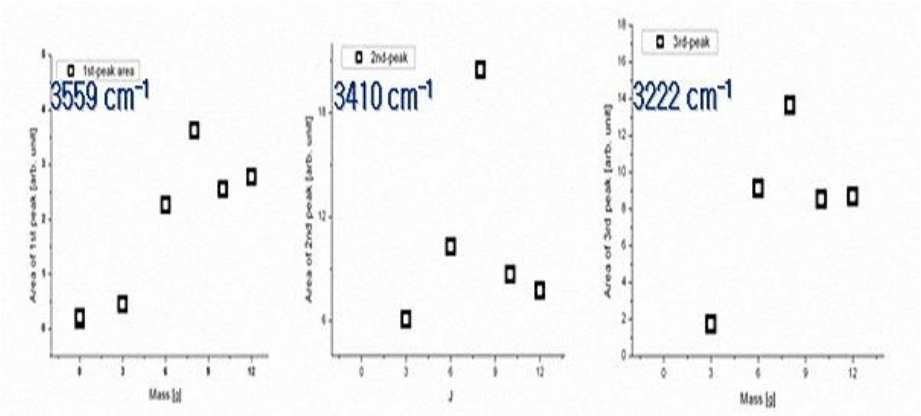

Fig. 6. Areas of Infrared Spectrum Absorbance (%) peaks for increasing amounts of Tourmaline (0g; 3g; 6g; 8g; 10g; 12g) with 0.5g H2O.

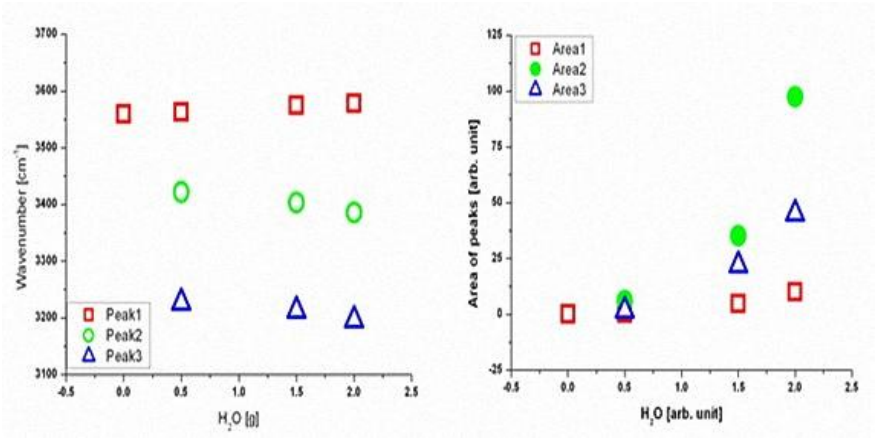

Fig. 7. Peak Positions and Areas of Infrared Spectrum Absorbance(%) peaks for increasing amounts of water (H2O) (0g; 0.5g; 1g; 2g) with 5g Tourmaline: 3559 cm-1 (red square), 3410 cm-1 (green circle), and 3222 cm-1 (blue triangle).

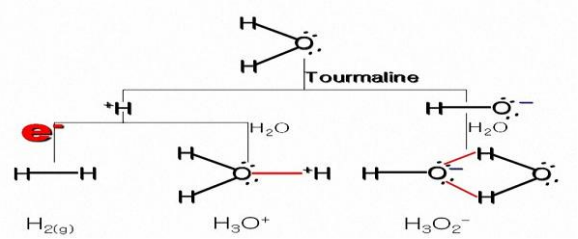

Fig. 8. Schematic diagrams of hydronium and hydroxyl ion formation by electrolysis of water.

Table 1
A simplified correlation FTIR chart of O-H functional group (Castaneda et al., 2006).

Type of vibration	Frequency (cm^{-1})	Intensity
Free	3600 ~ 3650	Medium
H-Bonded	3200 ~ 3500	Medium

Table 2
The pH measurements of 40ml H_2O and 5g Tourmaline at 19.8 °C.

Time	0 min	1 min	2 min	4 min
pH	6.86	9.90	9.96	9.98
Time	10 min	26 min	3 hours	≧8 hours
pH	9.91	9.97	9.4	9.90

4. Conclusion

The result regarding the tourmaline structures was verified through the Scanning Electron Microscopy (SEM), Energy Dispersive X-ray spectroscopy (EDX) analysis, and the X-ray Diffraction (XRD) analysis. The result regarding pyro-electricity was verified through the Infrared (IR) spectroscopy. We could see that the main structure of mixtures was consistent with the X-ray diffraction patterns of tourmaline and ferrite, respectively.

Through the FTIR experiments, we found how the electric field of the tourmaline played an important role in water activation. In Fig. 9, the water molecules produced electrolysis H^+ ion and HO^- ion after the tourmaline powder crystals contacted with water. The H^+ ion formed hydrogen gas (H_2) with free electron or hydronium ion (H_3O^+), and the hydroxy group (HO^- ion) formed $H_3O_2^-$, making water molecules appear alkaline. As other alkaline testaments, we measured the pH, which averaged 9.9, and the current, which was about -15.5 pA in the electric power saving system (Fig. 9).

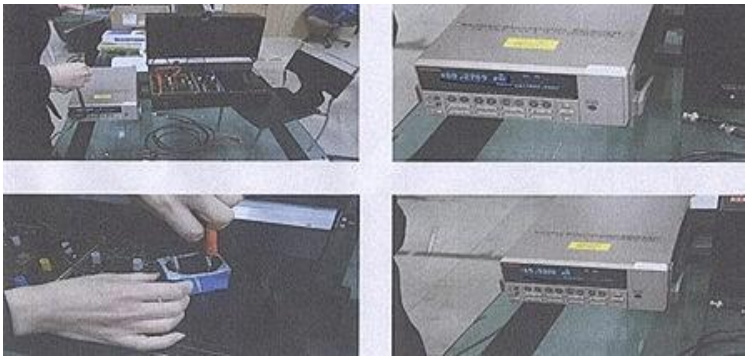

Fig. 9. Current flow as another alkaline testament.

Acknowledgments

This work was supported by the ENPOSS Institution and Hongik University. The FTIR curve fitting was achieved by Dr. Hwang, a professor in the physics department of Korea Air Force Academy. The author greatly thanks these contributors for their assistance and fellowship.

References

Bour, P., 2002. Chem. Phys. Lett., 365, 82.
Castaneda, C., Eeckhout, S.G., Costa, G.M., Boteho, N.F., Grave, E.D., 2006. Phys. Chem. Miner., 33(3), 207.
Choo, C.O., 2003. Geosci. J., 7(2), 151.
Dietrich, R.V., 1985. Van Nostrand Reinhold Company Inc., The Tourmaline Group. 13, 164.
Donny, G., Buerger, M.J., 1950. Acta Cryst., 3, 379.
Halmlin, A.C., 2011. The Tourmaline: The History of Mount Mica of Maine, U.S.A., Coachwhip Publications, 2009; Lauf, R.C.J. Collector's Guide to the Tourmaline Group, Schiffer.
http://www.mindat.org/min-4003.html.
Krambrock, K., Pinheiro, M.V.B., Guedes, K.J., Medeiros, S.M., Schweizer, S., Spaeth, J.M., 2004. Phys. Chem. Minerals, 31, 168.
Nemethy, G., Scheraga, H.A., 1962. J. Chem. Phys., 36(12), 3382.
Nishi, Y., Yazawa, Y., Oguri, K., Kanazaki, F., 1996. J. Intel. Mater. Syst. Struct., 7, 260.
Pavia, D.F., Lampman, G.M., Kriz, G.S., Jr., 1979. Introduction to Spectroscopy, Saunders, Co. 43.
Sun, S., Wei, C.D., Liu, Y.X.J., 2010. Nanoscience & Technology., 10, 2119.
Yvon, K., Jeitscho, W., Parthe, E.J., 1997. Appl. Cryst., 10, 73.
Zhu, D., Liang, J., Ding, Y., Xue, G., Liu, L.J., 2008. Am. Chem. Soc., 91(8), 2558.

How to cite this article: Chang, K.S., 2016. Pyroelectric study of Mongolian tourmaline in electric power saving system by infrared spectroscopy. Scientific Journal of Pure and Applied Sciences, 5(8), 476-482.